# The Kinetics of Methyl Loss from Ethylbenzene and Xylene Ions: The Tropylium versus Benzylium Story Revisited†

**Marcus Malow, Martin Penno, and Karl-Michael Weitzel***

*Institut für Chemie, Freie Universität Berlin, Takustrasse 3, 14195 Berlin, Germany*

*Received: April 1, 2003; In Final Form: August 13, 2003*

The rate constant curves $k(E)$ for the formation of $C_7H_7^+$ ions by methyl loss from energy selected ethylbenzene and *o*-xylene ions have been determined over a range from $10^3$ $s^{-1}$ to $5 \times 10^6$ $s^{-1}$ in a reflecting ion time-of-flight mass spectrometer. The observed threshold for methyl loss from ethylbenzene ions is 3 kJ/mol lower than that in *o*-xylene ions. The slope of the rate constant curves is very different at the threshold, indicating that isomerization of the precursors to a common intermediate does not play an important role. From the analysis we conclude that the $C_7H_7^+$ ions formed at the threshold have the structure of benzylium ions for ethylbenzene but that of tropylium ions for the *o*-xylene. At higher energies both $C_7H_7^+$ isomers appear to be formed from ethylbenzene ions.

## 1. Introduction

Despite the fact that $C_7H_7^+$ ions represent a textbook example of an important intermediate in organic mass spectrometry, its thermochemical properties have not been sufficiently well established for a long time.[1] The difficulty is related to the existence of three important isomers that may be formed (Scheme 1). It is now well accepted that the tropylium ion, first isolated by Döring and Knox[2] and investigated in the context of alkylbenzenes by Rylander et al.,[3] is the lowest energy isomer. However, its heat of formation, and that of the other isomers, are still disputed. For the $Tr^+$ ion the reference tables by Lias et al.[4] recommend a 0 K heat of formation of $\Delta_f H°(0K) = 872$ kJ/mol; for the $Bz^+$ ion the most accurate value available is $\Delta_f H°(0K) = 926$ kJ/mol,[5] i.e., about 54 kJ/mol above the $Tr^+$ ion. The heat of formation of the $To^+$ ion is less well-known. Indeed, the $To^+$ is believed to be formed in only few reactions, e.g., the loss of $NO_2$ from nitrotoluene ions. From photoelectron-photoion-coincidence (PEPICO) studies of the latter, Baer et al. derived $\Delta_f H°(0K) = 1094$ kJ/mol for the *p*-$Tol^+$ ion,[6] which is about 177 kJ/mol above the $Bz^+$ ion. For the fragmentation of alkylbenzenes in general only the formation of $Tr^+$ and $Bz^+$ appears to be relevant. Here one is interested in the following questions.

- Do the precursor ions isomerize prior to fragmentation?
- Which isomer is formed?
- What is the threshold energy for the formation of the different isomers?

For answering these questions one needs to be able to distinguish the product isomers. To some extent this is possible by secondary ion molecule reactions (collision-induced dissociation)[7] or by investigation of the kinetic energy release (KER).[8] The currently accepted view is that for the toluene ion ($Tol^+$) the experimental appearance energies for $Tr^+$ and $Bz^+$ are identical, i.e., the two reaction channels compete. This is supported by the observation of a large KER, indicating a reverse barrier for $Tr^+$ formation of about 30 kJ/mol.[8] There is some controversy on the ratio of $Tr^+/Bz^+$, with values ranging from about 3:1 at internal energies around 2.5 eV to about 0.7:1 above 5 eV.[1,9−11] Although the $Tr^+$ ion is thus believed to dominate in the near threshold fragmentation of $Tol^+$ ions, the fragmentation of *n*-propylbenzene ions[12] and *n*-butylbenzene ions[13] preferentially lead to $Bz^+$ ions.

**SCHEME 1: Structures of Three Important $C_7H_7^+$ Isomers: (a) Benzylium ($Bz^+$), (b) Tropylium ($Tr^+$), (c) Tolylium ($To^+$) (Only Para Isomer Shown)**

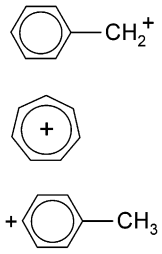


(a) (b) (c)

**SCHEME 2: Most Important Isomers of the $C_8H_{10}^+$ Ion: (d) Ethylbenzene Ion ($EtBz^+$), (e) 7−Methylcycloheptatrienyl Ion (Me-$CHT^+$), (f) *o*-Xylene Ion (*o*-$Xyl^+$) (Meta and Para Isomers Not Displayed)**

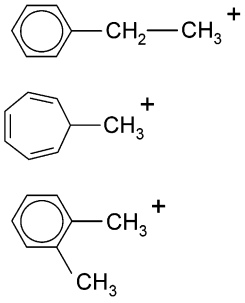


(d) (e) (f)

A key reaction system in this context is the ethylbenzene ion ($EtBz^+$), being intermediate between the toluene and *n*-propylbenzene ion. However, besides the $EtBz^+$ ion, two more important isomers of the $C_8H_{10}^+$ ion exist, as shown in Scheme 2 Here, the loss of $CH_3^•$ radicals from these $C_8H_{10}^+$ ions will lead

† Part of the special issue "Charles S. Parmenter Festschrift".

* Corresponding author. E-mail: weitzel@chemie.uni-marburg.de. Permanent address: Fachbereich Chemie, Philipps Universität Marburg, Hans-Meerweinstr., 35032 Marburg, Germany.

10.1021/jp0348427 CCC: $25.00 
Published on Web 10/11/2003

to the $C_7H_7^+$ ions discussed above. Again, the questions is, which isomer of the $C_7H_7^+$ is formed? Information on the reaction mechanism and thus on the structure of products can often be obtained from studies of $^{13}C$- and/or $^1D$-labeled precursors. An extensive investigation of various $^{13}C$- or $^1D$-labeled $EtBz^+$, Me-$CHT^+$, and $Xyl^+$ ions was reported by Grotemeyer and Grützmacher.[14] In a MIKES experiment employing EI ionization they found that for fragmentation at long reaction times (fragmentation in the second field free region) the carbon atoms are completely scrambled by skeletal rearrangement. At short reaction times (fragmentation in the ion source) the dynamics is dominated by hydrogen migration and a specific loss of terminal methyl groups.

In a recent MIKES study of the fragmentation of $EtBz^+$, Me-$CHT^+$, and *o*-, *m*-, and *p*-xylene$^+$ Kim and co-workers[15] found evidence for a bimodal kinetic energy release distribution (KERD). One component between 0 and 0.1 eV was assigned to the formation of $Bz^+$ ions; the other between 0.05 and 0.3 eV, to $Tr^+$ ions. A lower limit to the reverse barrier of $Tr^+$ ion formation of 5 kJ/mol was derived. DFT calculations of the same authors reveal that the threshold for formation of $Tr^+ + CH_3^\bullet$ occurs at 131.2 kJ above the ion ground state of $EtBz^+$. The threshold for formation of $Bz^+ + CH_3^\bullet$ on the other hand is believed to occur at 168 kJ relative to $EtBz^+$, i.e., about 37 kJ above the thermochemical $Tr^+$ threshold. Semiempirical calculations by Grotemeyer et al.[14] had led to an energy gap of 47 kJ. Both values are similar to the corresponding numbers in the toluene ion system. The transition states for interconversion of *p*-$Xyl^+$ to Me-$CHT^+$ and the transition state for the formation of $Tr^+$ are probably close to the threshold of $Bz^+$ ion formation.

Though the MIKES experiments referred to above have the advantage that the KER is in general dominated by the mechanism of the rate-determining step, the shortcoming is that the ions are not energy selected. Therefore, energy dependent characteristics are difficult to extract from such an approach. In this situation we see a need for experimental data on the fragmentation of $C_8H_{10}^+$ ions with well-defined internal energy. The current work reports such rate constant data for energy selected $EtBz^+$ and *o*-$Xyl^+$ ions as a function of the internal energy, with the goal to shed new light on the mechanism of tropylium and benzylium ion formation. The results will be compared to other available information from the literature.

## 2. Experimental Aspects

The fragmentation reactions of $EtBz^+$ and *o*-$Xyl^+$ ions have been investigated in a photoelectron-photoion-coincidence (PEPICO) spectrometer, which has been described in detail in previous work.[16] Only a brief overview focusing on the actual conditions of operation is given here. All experiments were carried out at room temperature in an effusive beam. The sample was ionized by dispersed synchrotron radiation from the 3 m NIM 1 beam line at the electron storage ring BESSY I at Berlin. To avoid any contribution from second-order light, a LiF window was utilized in all experiments.

The internal energy of the ions, $E_{int}$, is selected by detecting only threshold electrons, i.e., electrons with vanishing initial kinetic energy. It is given by the general formula for energy selection in coincidence experiments.[17,18]

$$E_{int} = h\nu + E_{th} - IE - E_{kin,e^-} \quad (1)$$

where $h\nu$ is the photon energy, $E_{th}$ is the thermal energy of the neutral sample, IE is the ionization energy, and $E_{kin,e^-}$ is the kinetic energy of the electron. The threshold energy analysis is performed in a static field of 4.6 V/cm. Only after detection of an electron is a field pulse of 466 V/cm switched on to draw the corresponding ion out of the ion source. Consequently, the ions are analyzed in a reflecting ion time-of-flight mass spectrometer (reflectron).[16,19] The total kinetic energy of the ions is 1300 V. The ion time-of-flight coincidence (RETOF) spectra are obtained by using the electron signal as the start and the ion signal as a stop of the ion time-of-flight measurement. The total energy resolution of the experiment was 15 meV.

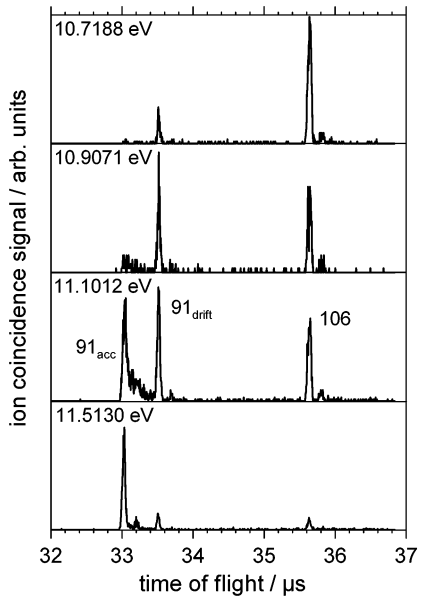


**Figure 1.** RETOF spectra of ethylbenzene at various excitation energies. Note, only the principal ions are labeled, but not the $^{13}C$ isotopomers.

Ethylbenzene and *o*-xylene were obtained from Aldrich and degassed by several freeze cycles before use.

## 3. Results and Discussion

The fragmentation of energy selected $EtBz^+$ and *o*-$Xyl^+$ ions has been investigated in the photon energy range between about 10.7 and 11.7 eV. The RETOF mass spectra for the $EtBz^+$ and the *o*-$Xyl^+$ are shown in Figures 1 and 2, respectively. For both precursor molecules at low excitation energy the parent ion (and its $^{13}C$ isotopomer) dominate. With increasing photon energy the amount of fragmentation increases. For the energy range discussed in this work the $EtBz^+$ ions exclusively decay by methyl loss, leading to the $C_7H_7^+$ ion. This reaction channel also clearly dominates in the *o*-Xyl data. However, at the highest energies a small fraction of H loss is observed from the xylene ions (<5%). For the fragment ion of interest, the $m/z = 91$ ion, the spectra in Figures 1 and 2 exhibit 2 peaks. The left peak labeled $91_{acc}$ originates from fragmentation events in the ion source; the right one, labeled $91_{drift}$, originates from fragmentation in the first field free region. In fact, the ability to identify fragmentation events in the drift region represents the major advantage of a reflectron over a linear TOF-MS, leading to an increased sensitivity for small $k(E)$ values.

From first glance we notice that the drift ion signal, often termed the metastable signal, extends over a larger range of energy in *o*-$Xyl^+$ compared to $EtBz^+$. This already indicates that the slopes of the rate constant curves $k(E)$ are most likely different for the two precursors. For a more detailed analysis we have extracted the fractional abundance of ions formed in the ion source ($FA_{acc}$), the drift region ($FA_{drift}$), and preserved ions ($FA_{parent}$) from the RETOF spectra.

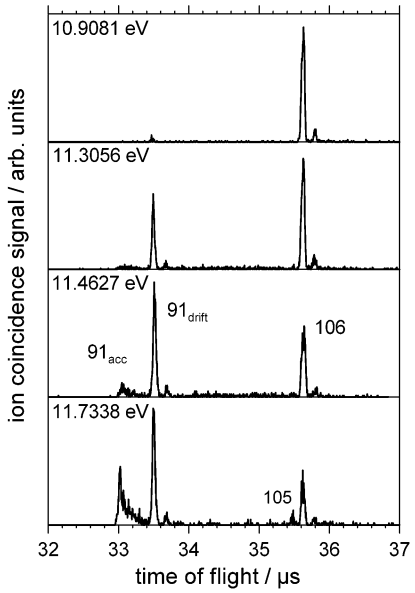


**Figure 2.** RETOF spectra of *o*-xylene at various excitation energies. Note, only the principal ions are labeled, but not the $^{13}C$ isotopomers.

$$F_{i,m} = \frac{Y_{i,m}}{\sum_i \sum_m Y_{i,m}} \quad (2)$$

where i designates the region in which the ion is formed (omitted in the case of the parent ion) and $m$ is the mass of the ion. For EtBz the analysis includes $F_{acc,91}$, $F_{drift,91}$, and $F_{106}$. For *o*-Xyl the $m/z = 105$ ion signal (i.e., the H loss reaction) is included in addition.

These normalized fractional abundances are plotted in breakdown diagrams for EtBz (Figure 3) and *o*-Xyl (Figure 4). Again we note that at small photon energy the parent ion dominates, although for EtBz even at 10.7 eV about 15% of the precursor ions dissociate. With increasing photon energy, the metastable drift ion signal increases. For EtBz this signal runs through a maximum around 11 eV and decreases again toward higher energy. For *o*-Xyl the range over which the drift ion signal is observed is significantly larger with a broad maximum around 11.55 eV. For *o*-Xyl the most intense ion signal around 11.7 eV is the drift ion signal $m/z = 91$ (49%), whereas for EtBz it is the prompt ion signal $m/z = 91$ (85%).

In the following section we describe the derivation of complete rate constant curves $k(E)$ from a detailed analysis of the breakdown curves (Figures 3 and 4). For this purpose we calculated the breakdown diagrams directly from molecular parameters using the rate constant curves as adjustable parameters. As discussed in more detail in previous work,[20−22] the observed fractional abundances FA can be calculated from

$$\mathrm{FA}_{i,calc}(h\nu) = \sum_{E_{th}} \sum_{E_{el}} F_i(E_{int})\ \mathrm{TPES}(E_{int})\ \mathrm{If}(E_{kin,e^-})\ P(E_{th}) \quad (3)$$

where $\mathrm{If}(E_{kin,e^-})$ is the instrument function, $P(E_{th})$ is the energy distribution of the thermal sample, and $F_i(E_{int})$ are the molecular fractional abundances. The ion internal energy is given by eq 1. The instrument function takes into account the amount of electrons with kinetic energy traveling through the steradiancy analyzer without being discriminated. The experimental instrument function can be determined, for example, from the threshold photoelectron spectrum (TPES) of argon in the region

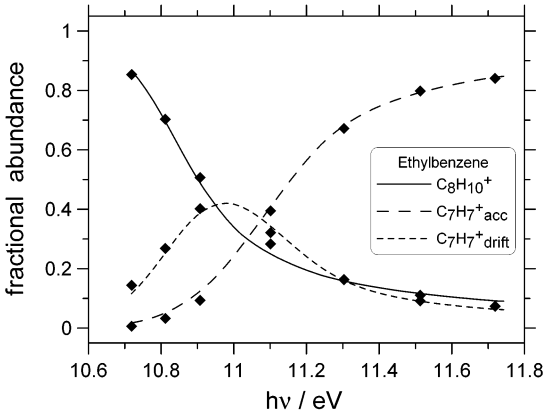


**Figure 3.** Breakdown curves of ethylbenzene: symbols, experimental data; lines, calculated data.

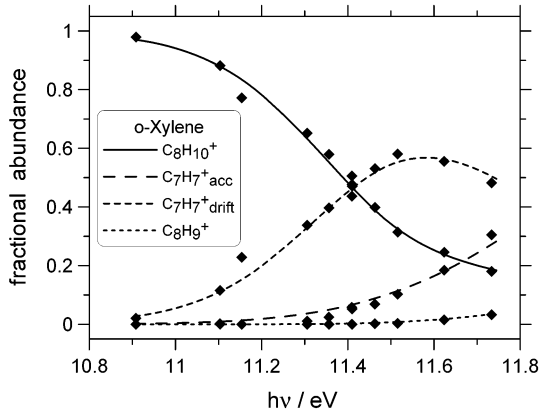


**Figure 4.** Breakdown curves of *o*-xylene: symbols, experimental data; lines, calculated data.

of the $^2P_{1/2}$ state. The thermal energy distribution of the sample is calculated from $P(E_{th}) = N(E_{vr}) \exp[-E_{vr}/kT]$,[20] where $N(E_{vr})$ are the rovibrational density of states based on the vibrational frequencies for EtBz[23] and *o*-Xyl.[24]

The molecular fractional abundance $F_i(E_{int})$ directly depends on the rate constants, as described below. First we discuss the fragmentation leading to products in a single first-order step (applies to the EtBz). Here, the molecular fractional abundances are given by

$$F_{acc}(E_{int}) = 1 - e^{-k(E_{int})t_{acc}} \quad (4)$$

$$F_{drift}(E_{int}) = e^{-k(E_{int})t_{acc}} - e^{-k(E_{int})(t_{acc}+t_{drift})} \quad (5)$$

$$F_{parent}(E_{int}) = e^{-k(E_{int})(t_{acc}+t_{drift})} \quad (6)$$

where $t_{acc}$ and $t_{drift}$ are the residence times of the parent ion in the different regions of the spectrometer and $k(E_{int})$ is the rate constant leading to this particular fragment ion with fractional abundances $F_{acc}$ and $F_{drift}$. In the case of two competing reaction channels leading to ions 1 and 2 (applies to the *o*-Xyl) with rate constants $k_1$ and $k_2$, the molecular fractional abundances are given by

$$F_{acc,1}(E_{int}) = \frac{k_1(E_{int})}{k_1(E_{int}) + k_2(E_{int})}(1 - e^{-(k_1(E_{int})+k_2(E_{int}))t_{acc}}) \quad (7)$$

$$F_{acc,2}(E_{int}) = \frac{k_2(E_{int})}{k_1(E_{int}) + k_2(E_{int})}(1 - e^{-(k_1(E_{int})+k_2(E_{int}))t_{acc}}) \quad (8)$$

$$F_{\text{drift},1}(E_{\text{int}}) = \frac{k_1(E_{\text{int}})}{k_1(E_{\text{int}}) + k_2(E_{\text{int}})}(e^{-k_{\text{tot}}(E_{\text{int}})t_{\text{acc}}} - e^{-k_{\text{tot}}(E_{\text{int}})(t_{\text{acc}}+t_{\text{drift}})}) \quad (9)$$

$$F_{\text{drift},2}(E_{\text{int}}) = \frac{k_2(E_{\text{int}})}{k_1(E_{\text{int}}) + k_2(E_{\text{int}})}(e^{-k_{\text{tot}}(E_{\text{int}})t_{\text{acc}}} - e^{-k_{\text{tot}}(E_{\text{int}})(t_{\text{acc}}+t_{\text{drift}})}) \quad (10)$$

$$F_{\text{parent}}(E_{\text{int}}) = e^{-k_{\text{tot}}(E_{\text{int}})(t_{\text{acc}}+t_{\text{drift}})} \quad (11)$$

where the total rate constant $k_{\text{tot}} = k_1 + k_2$. In the hypothetical case of an experiment at 0 K and infinite resolution, the molecular fractional abundances $F_i$ would be identical to the observable fractional abundances $FA_i$. In the analysis of the experimental data, the rate constant curves are adjusted until the best agreement between calculated and experimental breakdown data is obtained. These calculated breakdown curves are also shown in Figure 3 for EtBz and in Figure 4 for *o*-Xyl. Within the experimental uncertainty the agreement is very good for both the EtBz and the *o*-Xyl.

Finally, we have to present the rate constant curves obtained from this analysis. First we concentrate on the specific rate constants for methyl loss from $EtBz^+$ and *o*-$Xyl^+$ ions, which are shown in Figure 5. To be able to compare the two rate constant curves on an absolute energy scale, we use the sum of ion internal energy, ionization energy, and the heat of formation of the respective neutral as the abscissa. This allows to identify processes occurring at the same absolute energy. The following values were employed: IE(EtBz) = 8.77 eV,[4] IE(*o*-Xyl) = 8.56 eV,[4] $\Delta_f H$(EtBz,0K) = 60.6 kJ/mol.[15] The 298 K heat of formation for *o*-Xyl is identical to that for *p*-Xyl.[4] For the 0 K heat of formation of *o*-Xyl required in this context we therefore employed the most recent value from Kim et al., $\Delta_f H$(*p*-Xyl,0K) = 45.5 kJ/mol.[15]

Before discussing the results, we have to point out the limits of sensitivity of our analysis. For the EtBz the analysis is sensitive to the rate constant between about $2 \times 10^3$ $s^{-1}$ and about $5 \times 10^6$ $s^{-1}$. For the *o*-Xyl the sensitive range is between about $10^3$ and $10^6$ $s^{-1}$. The limitation at high rate constants for *o*-$Xyl^+$ originates from the fact that the metastable peak range for *o*-Xyl is not completely covered toward the high energy side. The latter was due to intensity problems in approaching the cutoff of the LiF window used (in our setup: <11.8 eV). For the $EtBz^+$ ion the metastable peak range is not completely covered toward the low energy side. From Figure 5 we note that the experimental onset of the $k(E)$ curve for $CH_3$ loss is 3 kJ/mol smaller in the EtBz compared to the *o*-Xyl. Due to the limitation of detecting rate constants smaller than about $10^3$ $s^{-1}$, the true molecular threshold energy is most likely smaller in *o*-Xyl. The slope of the two $k(E)$ curves represents one central result of this work. Note that the energy resolution of the experiment is on the order of 15 meV, i.e., about 1.45 kJ/mol.

The fact that the slope of the $k(E)$ curves in the threshold region is much larger for $EtBz^+$ compared to *o*-$Xyl^+$, gives direct evidence that isomerization to a common intermediate cannot be relevant for this process. It rather indicates that the fragmentation of $EtBz^+$ ions and *o*-$Xyl^+$ ions leads to different isomers of the $C_7H_7^+$ ion at the threshold. We conclude that under the conditions of our experiment most likely $Bz^+$ is formed from $EtBz^+$ but the $Tr^+$ ion is formed from *o*-$Xyl^+$ at threshold. Interestingly, at higher internal energy the slope of the two $k(E)$ curves appears to become comparable. We will come back to this aspect.

In the previous section the absolute energy scale was chosen for the comparison of EtBz and *o*-Xyl data. More often, rate constant data are presented as a function of the internal energy of the parent molecules. In fact, the entire analysis is based on a numerical solution of eq 3 in the domain of ion internal energy. For comparison to other results from the literature, particularly those in a different energy range, it is most helpful to also have an analytical representation of the $k(E)$ data. This will be discussed in the following section.

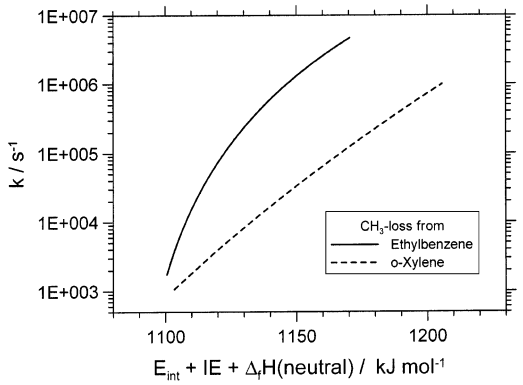


**Figure 5.** Rate constant curves for the methyl loss from ethylbenzene and *o*-xylene ions. Note the use of an absolute thermodynamic energy axis.

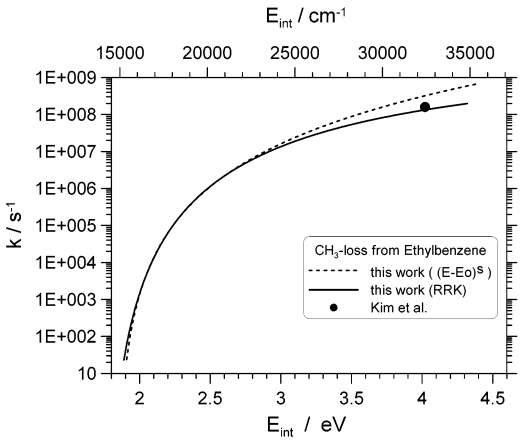


**Figure 6.** Rate constant data for the methyl loss from ethylbenzene ions as a function of the ion internal energy: lines, this work (for the different models, see text); symbol, experiment. Data from ref 15. Compare to Figure 5 for sensitivity range of the current experiment.

For the extrapolation of the EtBz data to lower and higher energies, we have employed two different approaches. The first one is based on an intriguingly simple formula suggested by Troe.[25] Adopting the form also employed by Troe et al.[26] in recent work, we are now able to represent our $k(E)$ data for methyl loss from $EtBz^+$ by the following parametrized equation

$$k(E_{\text{int}}) = 1.6 \times 10^8 \left(\frac{E_{\text{int}} - 14843}{15178}\right)^{4.7337} \quad (12)$$

where the energies are in $cm^{-1}$ in accordance with the standard convention and $k(E)$ is given in units of $s^{-1}$. In eq 12 the number 14843 is a fit parameter being not far from the threshold energy in $cm^{-1}$. In Figure 6 this $k(E)$ curve is plotted over an extended energy range (both for eV and $cm^{-1}$). Kim et al.[15] have reported a single value of $k = (1.6 \pm 0.4) \times 10^8$ $s^{-1}$ obtained by photodissociation at an effective internal energy of 4.02 eV. For comparison this data point is included in Figure 6. We note that the $k(E)$ curve derived in this work would lead to a $k(E)$ of $3.2 \times 10^8$ $s^{-1}$ at 4.02 eV, i.e., 2 times the value of Kim et al. For this reason we have also attempted to extrapolate our $k(E)$

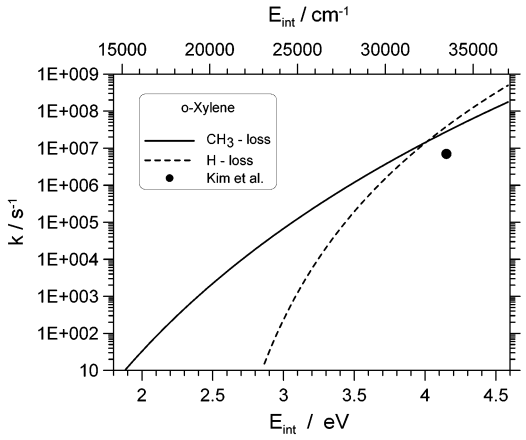


**Figure 7.** Rate constant curves for the methyl loss and H loss from *o*-xylene ions as a function of the ion internal energy: lines, this work; symbol, experiment. Data from ref 15. Compare to Figure 5 for sensitivity range of the current experiment.

data by a classical RRK approach. Here the following equation fits our experimental data equally well

$$k(E_{\text{int}}) = 9.74 \times 10^{9}\left(\frac{E_{\text{int}} - 14159}{E_{\text{int}}}\right)^{7.4742} \qquad (13)$$

This second $k(E)$ curve is also shown in Figure 6. We note that this curve fits much better to the single data point from Kim et al., the actual value at 4.02 eV being $1.3 \times 10^{8}$ s$^{-1}$. The number of 14 156 is again a fit parameter, being not far from the threshold energy. We will come back to this point in the discussion.

For the methyl loss from *o*-Xyl$^+$ the rate constant curve was expressed as

$$k(E_{\text{int}}) = 1.542 \times 10^{8}\left(\frac{E_{\text{int}} - 955.03}{35768.775}\right)^{17.9297} \qquad (14)$$

In addition to the methyl loss we have also been able to extract a $k(E)$ curve for the H loss from *o*-Xyl$^+$ ions, which can be represented by the following expression:

$$k(E_{\text{int}}) = 1.012 \times 10^{9}\left(\frac{E_{\text{int}} - 18883.29}{19183.67}\right)^{11.9049} \qquad (15)$$

These two specific $k(E)$ curves are plotted in Figure 7, indicating the energy axis both in cm$^{-1}$ and in eV. Again a single value of $k(E) = (7 \pm 3) \times 10^{6}$ s$^{-1}$ for methyl loss, measured by Kim et al.[15] at an effective internal energy of 4.15 eV, has been included in Figure 7. At that internal energy our value would be $2.7 \times 10^{7}$ s$^{-1}$. We were unable to represent our $k(E)$ data for the *o*-Xyl$^+$ by a classical RRK approach. Note that eqs 12−15 are empirical fit expressions to be validated by true theoretical treatments. The uncertainty of our $k(E)$ data for methyl loss is estimated to be on the order of ±30%, for the H loss it is on the order of ±50%.

## 4. Summary and Discussion

We have measured the breakdown curves of ethylbenzene (EtBz) and *o*-xylene (*o*-Xyl) in a PEPICO experiment. For EtBz only methyl loss is observed in the energy range covered; for *o*-Xyl methyl loss as well as H loss are observed. For all three processes complete rate constant curves have been derived in the range between about $10^{3}$ s$^{-1}$ and $5 \times 10^{6}$ s$^{-1}$. Our $k(E)$ curves are in reasonable agreement with data from Kim et al.,[15] considering that our experimental data are derived at significantly smaller internal energies. The current work represents one of only a few examples of direct $k(E)$ measurements down to values around $10^{3}$ s$^{-1}$.[27] This became possible by the combination of the PEPICO technique with a reflectron.

The slope of the two $k(E)$ curves for methyl loss from EtBz$^+$ and *o*-Xyl$^+$ ions is significantly different in the threshold region. From this we conclude that methyl loss does not take place from a common intermediate, i.e., isomerization of the precursor molecule does not play a major role, at threshold. From the extrapolation of our experimental $k(E)$ data to lower energy we obtain information on the true dissociation energy of the EtBz$^+$ ion. From the Troe formula we arrive at Eo = 14 843 cm$^{-1}$; from a classical RRK approach we arrive at Eo = 14 156 cm$^{-1}$. The latter is in almost perfect agreement with the most accurate current information from Ellison et al.[5] Combining $\Delta_f H$(Bz$^+$,0K) = 926 kJ/mol,[5] $\Delta_f H$(CH$_3$,0K) = 149 kJ/mol,[4] and $\Delta_f H$(EtBz$^+$,0K) = 907 kJ/mol,[15] we arrive at a dissociation energy of the EtBz$^+$ ion with respect to Bz$^+$ + CH$_3$ of Eo = 168 kJ/mol, i.e., 14 044 cm$^{-1}$. Our Eo = 14 156 cm$^{-1}$, derived from the RRK representation comes remarkably close to this value. However, given the simplicity of the $k(E)$ approach, we do not want to over interpret this nice agreement.

In any case this thermochemical consideration provides strong evidence for the conclusion, that the $C_7H_7^+$ ion formed at threshold from EtBz$^+$ has the Bz$^+$ structure. For the methyl loss from *o*-Xyl$^+$ ions it is not possible to extract a threshold energy from the experimental data. This is partly due to the very small curvature of the log $k(E)$ curve, which does not allow us to extrapolate to the threshold energy, unless the threshold rate constant would become available. From what is known in the literature[4] the heat of formation of the *o*-Xyl$^+$ ion is about 40 kJ/mol lower than that of EtBz$^+$. Assuming the *o*-Xyl$^+$ ions also form the Bz$^+$ ion at threshold would require a rate constant much smaller than observed in our experiment. Combined with the observation of a distinctly different slope of the $k(E)$ curve, we conclude that the $C_7H_7^+$ ion formed at threshold from *o*-Xyl$^+$ most likely has the Tr$^+$ structure. At higher energy the slope of the $k(E)$ curves for methyl loss from the two precursors becomes comparable. In principle, this might indicate isomerization to a common intermediate. However, this seems to be discarded by two arguments. First, the absolute rate constants $k(E)$ differ by about 2 orders of magnitude at absolute energies above 1120 kJ/mol. Second, the amount of H loss reaction observed is higher in *o*-Xyl compared to EtBz. In the *o*-Xyl experiment the fractional abundance of $C_8H_9^+$ ions (due to H loss) is about 3.5% at 11.73 eV, and about 5.3% at 12.155 eV (not shown in Figure 4). In the EtBz experiment there is no indication of H loss below 11.6 eV. At 12.155 eV H loss accounts for about 2.7% of the total signal (not shown in Figure 3). Thus at a given excitation energy H loss from *o*-Xyl$^+$ ions is a factor of 2 more intense then in EtBz$^+$.

Another possible interpretation of the high energy data is related to the problem of isomerization. There is experimental evidence that at sufficiently high internal energy precursor ions and even fragment ions may isomerize.[14,28] If the barrier for isomerization of the precursor molecule is low compared to the dissociation threshold or the relevant internal energy is high above that barrier, then the fragmentation dynamics is probably not influenced by the isomerization dynamics. For the EtBz/*o*-Xyl system, however, all available information suggests that the barrier for isomerization of EtBz$^+$ to Me-CHT$^+$ is almost isoenergetic to the threshold for methyl loss.[14,15] However, most likely the barrier for isomerization of the xylene ions to the

Me-$CHT^+$ is slightly smaller than the former. In this situation it does not seem probable that the isomerization barriers can cause the $k(E)$ from *o*-$Xyl^+$ to be about 2 orders of magnitude smaller than that from $EtBz^+$.

On the absolute energy scale the observed threshold energy is 3 kJ/mol higher in *o*-$Xyl^+$ ions compared to $EtBz^+$ ions. This threshold is given by the smallest rate constant to which our experiment is sensitive. Thus the values are most likely still influenced by some kinetic shift. The absolute threshold for methyl loss from $EtBz^+$ is observed at 1100.5 kJ/mol and that for methyl loss from *o*-$Xyl^+$ is observed at 1103.5 kJ/mol. Employing the 0 K heat of formation for $Bz^+$ (926 kJ/mol) from Ellison et al.[5] and the methyl radical (149.0 kJ/mol) from Lias et al.,[4] we expect the threshold for $Bz^+$ formation at 1075 kJ/mol, i.e., 25.5 kJ/mol below our observed onset. However, as discussed above, the extrapolation of our measured $k(E)$ data to the threshold would lead to a threshold energy of 1076 kJ/mol in nice agreement with the former value. The thermochemical threshold for the formation of $Tr^+$ would be expected at 1021 kJ/mol.[4] However, as mentioned before, there seems to be a considerable reverse barrier for $Tr^+$ formation, which is probably on the order of 30 kJ/mol. This leads to an estimated threshold energy of about 1051 kJ/mol, still 52.5 kJ/mol below our measured onset of the $k(E)$ curve. From the analysis of the EtBz data it is evident that our experiment is subject to some kinetic shift. Nevertheless, the discrepancy between our observed onset and the expected threshold seems very large in the case of *o*-Xyl.

Finally, the results of the current work can be compared to work on the competition between fragmentation and energy transfer in $EtBz^+$ ions formed by chemical ionization.[29] Here, the recent analysis of the kinetic data currently available indicates a turn over from phase space behavior at low internal energy to valence-determined behavior at high internal energy.[26] This appears to be fully consistent with our conclusion, that the formation of $Bz^+$ ions via a simple bond cleavage dominates at low internal energy. Even at higher internal energies around 4 eV the most recent results suggest[30] that the $Tr^+$ channel does not account for more than 5−10% of the total product yield.

## Appendix

In this appendix we list the vibrational frequencies used in the calculation of the thermal energy distribution of the sample:

Ethylbenzene:[23] 3061, 3055, 3049, 3043, 3038, 2965, 2965, 2918, 2878, 2855, 1606, 1589, 1500, 1467, 1459, 1455, 1453, 1378, 1332, 1310, 1310, 1245, 1207, 1179, 1157, 1072, 1065, 1033, 1021, 1003, 990, 975, 967, 904, 856, 787, 771, 749, 700, 618, 557, 487, 415, 362, 314, 219, 157, 30.

*o*-Xylene:[24] 3063, 3054, 3045, 3041, 2940, 2939, 2938, 2938, 2927, 2927, 1618, 1591, 1487, 1456, 1456, 1456, 1454, 1447, 1392, 1388, 1296, 1269, 1223, 1205, 1166, 1133, 1044, 1043, 1028, 982, 975, 966, 935, 862, 831, 740, 735, 704, 562, 501, 499, 432, 400, 246, 241, 175, 157, 154.

**Acknowledgment.** Financial support of this work by the Deutsche Forschungsgemeinschaft is gratefully acknowledged. We cordially thank Prof. J. Troe for stimulating discussions and careful reading of the manuscript.

## References and Notes

(1) Lifshitz, C. *Acc. Chem. Res.* **1994**, *25*, 138.
(2) Döring, W. von E.; Knox, L. H. *J. Am. Chem. Soc.* **1954**, *76*, 3203.
(3) Rylander, P. N.; Meyerson, S.; Grupp, M. M. *J. Am. Chem. Soc.* **1957**, *79*, 842.
(4) Lias, S. G.; Bartmess, J. E.; Liebmann, J. F.; Holmes, J. L.; Levin, R. D.; Mallard, W. G. *J. Phys. Chem. Ref. Data* **1988**, 17, Suppl. 1.
(5) Ellison, G. B.; Davico, G. E.; Bierbaum, V. M.; DePuy, C. H. *Int. J. Mass Spectrom. Ion Processes* **1996**, *156*, 109.
(6) Baer, T.; Morrow, J. C.; Shao, J. D.; Olesik, S. *J. Am. Chem. Soc.* **1988**, *110*, 5633.
(7) Olesik, S.; Baer, T.; Morrow, J. C.; Ridal, J. L.; Buschek, J.; Holmes, J. L. *Org. Mass Spectrom.* **1989**, *24*, 1008.
(8) Moon, J. H.; Choe, J. C.; Kim, M. S. *J. Phys. Chem. A* **2000**, *104*, 458.
(9) Lifshitz, C.; Gotkis, Y.; Ioffe, A.; Laskin, J.; Shaik, S. *Int. J. Mass Spectrom. Ion Processes* **1993**, *125*, R7.
(10) Dunbar, R. C. *J. Am. Chem. Soc.* **1975**, *97*, 1382.
(11) Ausloos, P. *J. Am. Chem. Soc.* **1982**, *104*, 5259.
(12) Hwang, W. G.; Moon, J. H.; Choe, J. C.; Kim, M. S. *J. Phys. Chem. A* **1998**, *102*, 7512.
(13) Oh, S. T.; Choe, J. C.; Kim, M. S. *J. Phys. Chem.* **1996**, *100*, 13367.
(14) Grotemeyer, J.; Grützmacher, H.-Fr. *Org. Mass Spectrom.* **1982**, *17*, 353.
(15) Kim, Y. H.; Choe, J. C.; Kim, M. S. *J. Phys. Chem. A* **2001**, *105*, 5751.
(16) Güthe, F.; Malow, M.; Weitzel, K.-M.; Baumgärtel, H. *Int. J. Mass Spectrom. Ion Processes* **1998**, *172*, 47.
(17) Baer, T.; Booze, J. A.; Weitzel, K.-M. In *Vacuum Ultraviolet Photoionization and Photodissociation of Molecules and Clusters*; Ng, C. Y., Ed.; World Scientific: Singapore, 1991.
(18) Weitzel, K.-M. *Trends Chem. Phys. Res.* **1997**, *6*, 143.
(19) Güthe, F.; Weitzel, K.-M. *Ber. Bunsen-Ges. Phys. Chem.* **1997**, *101*, 484.
(20) Weitzel, K.-M.; Booze, J.; Baer, T. *Chem. Phys.* **1991**, *150*, 263.
(21) Weitzel, K.-M.; Booze, J.; Baer, T. *Int. J. Mass Spectrom. Ion Processes* **1991**, *107*, 301.
(22) Weitzel, K.-M. In *Photoionization and Photodetachment*; Ng, C. Y., Ed.; Advances in Physics and Chemistry Series; World Scientific Publishing: Singapore, 2000; p 539.
(23) Snyder, R. W.; Painter, P. C. *Polymer* **1981**, *22*, 1629.
(24) Draeger, J. *Spectrochim. Acta* **1985**, *41A*, 607.
(25) Troe, J. *J. Phys. Chem.* **1983**, *87*, 1800.
(26) Troe, J.; Viggiano, A. A.; Williams, S. *J. Phys. Chem. A* submitted for publication.
(27) Weitzel, K.-M. *Ber. Bunsen-Ges. Phys. Chem.* **1998**, *102*, 989.
(28) Buschek, J. M.; Ridal, I. J.; Holmes, J. L. *Org. Mass Spectrom.* **1988**, *23*, 543.
(29) Viggiano, A. A.; Miller, T. H.; Williams, S.; Arnold, S. T.; Seely, J. V.; Friedman, J. F. *J. Phys. Chem. A* **2002**, *106*, 11917.
(30) Troe, J. Private communication; see also ref 43 of ref 26 above.